Climatic Change (2015) 132:237–249
DOI 10.1007/s10584-015-1419-x

Increasing Northern Hemisphere water deficit

Gregory J. McCabe[1] **· David M. Wolock**[2]

Received: 21 November 2014 / Accepted: 26 April 2015 / Published online: 5 May 2015

Abstract A monthly water-balance model is used with CRUTS3.1 gridded monthly precipitation and potential evapotranspiration (PET) data to examine changes in global water deficit (PET minus actual evapotranspiration) for the Northern Hemisphere (NH) for the years 1905 through 2009. Results show that NH deficit increased dramatically near the year 2000 during both the cool (October through March) and warm (April through September) seasons. The increase in water deficit near 2000 coincides with a substantial increase in NH temperature and PET. The most pronounced increases in deficit occurred for the latitudinal band from 0 to 40°N. These results indicate that global warming has increased the water deficit in the NH and that the increase since 2000 is unprecedented for the 1905 through 2009 period. Additionally, coincident with the increase in deficit near 2000, mean NH runoff also increased due to increases in P. We explain the apparent contradiction of concurrent increases in deficit and increases in runoff.

1 Introduction

The increase in global temperatures during the past several decades has raised concerns about potential effects of global warming on hydrologic conditions (Gleick 2000; Nijssen et al. 2000; Arnell 2003; Milly et al. 2005; Intergovernmental Panel on Climate Change 2014). For example, Nijssen et al. (2000) examined changes in streamflow resulting from climate projections for 2025 and 2045. They found that, in general, streamflow increased in high-latitude basins and decreased in tropical basins. In a later study, Arnell (2003) examined changes in river flow for sites across the globe using climate projections from six GCMs. Similar to the Nijssen et al. (2000) study, Arnell (2003) found that streamflow increased for high latitude basins. Arnell (2003) also reported decreases in streamflow for mid-latitude basins and a mixture of increases and decreases in streamflow in tropical areas. Milly et al. (2005) examined changes in streamflow projected by 12 climate models for the year 2050. Milly et al. (2005) reported 10–40 percent (%) increases in streamflow in eastern equatorial

✉ Gregory J. McCabe
gmccabe@usgs.gov

[1] U.S. Geological Survey, Denver Federal Center, MS 412, Denver, CO 80225, USA

[2] U.S. Geological Survey, Lawrence, KS, USA

Africa, the La Plata basin in southern South America, and in high-latitude North America and Eurasia, as well as 10–30 % decreases in streamflow in southern Africa, southern Europe, the Middle East, and mid-latitude western North America.

In a study of changes in global water balance components during 1905–2009, McCabe and Wolock (2014) reported that precipitation (P) has been the primary driver of variability in streamflow. Additionally, the study showed that since about 2000, there have been increases in P, actual evapotranspiration (AET), streamflow (Q), and potential evapotranspiration (PET) for most of the globe. The increases in Q during 2000 through 2009 have occurred despite unprecedented increases in PET. The increases in Q are the result of substantial increases in P during the cool Northern Hemisphere months (i.e., October through March) when PET increases were relatively small; the largest PET increases occurred during the warm Northern Hemisphere months (April through September).

A number of previous studies have indicated an increase in global aridity (i.e., climatic dryness) and risk of drought (Rind et al. 1990; Wang 2005; Dai et al. 2004; Seager et al. 2007; Burke and Brown 2008; Sheffield and Wood 2008; Dai 2011, 2013). These studies examined changes in precipitation, streamflow, and drought indices (e.g., Palmer Drought Severity Index (PDSI)), but none used water deficit (D), defined below, which is a variable of the water balance.

Precipitation and PET are the most basic drivers of the water balance. Precipitation (P) comprises the climatic supply of water at a location and PET represents the climatic demand for water at a location. The balance between these two variables determines water availability for Q and AET. The relation between P and PET also is often used to compute moisture and aridity indices for climate classification (Budyko 1948; Willmott and Feddema 1992; Arora 2002; Weiskel et al. 2014). An interesting and important water balance residual that has not received much attention in the climate change literature is deficit (D). Deficit is defined as the climatic demand for water (i.e., PET) that is in excess of AET.

Deficit integrates two fundamental climate factors (precipitation and temperature) and represents a biologically relevant variable that accounts for the simultaneous availability of water and energy (Stephenson 1990; Dobrowski et al. 2013). It has greater physiological relevance to plants than do standard climatic variables such as temperature and precipitation (Stephenson 1990). Previous research has shown that the variability of deficit is associated with variability in soil-moisture storage and irrigation needs (McDonald and Girvetz 2013), variability of vegetation types (Stephenson 1998), changes in the location and occurrence of losing streams (Weiskel et al. 2014), and changes in the proportions of green and blue water (Weiskel et al. 2014). Green water is water that is evaporated and not available for human use, whereas blue water is water that generates streamflow and water supplies (Falkenmark and Rockstrom 2006; Weiskel et al. 2014). Thus, changes in deficit can have substantial implications for agriculture, irrigation needs, and natural vegetation. Deficit may be one of the best indicators of agricultural drought that results from decreased precipitation and/or increased evaporation, both of which result in reduced crop yields and plant growth. (Dai 2011).

The objectives of this study are to (1) examine changes in Northern Hemisphere (NH) deficit during the past century, (2) identify regions in the NH that have experienced increases in water deficit, and (3) place magnitudes of recent deficit values in the context of historical deficit values during the past century.

2 Data and methods

Monthly P and PET data for the globe were obtained from the Climate Research Unit (CRU) at East Anglia, United Kingdom dataset [the CRUTS3.10 dataset]. The spatial resolution of this dataset, which covers the land areas of the globe, is 0.5 degree (°) by 0.5° and spans the period 1901 through 2009. Because a majority of global land area (~74 %) is in the Northern Hemisphere (NH), our analyses use data for just the NH. Additionally, data poleward of 70° North latitude were not used because many of the monthly P and PET values for these grid cells were generated from sparse meteorological observations; focusing on the NH and excluding data poleward of 70° North latitude left 44832 grid cells for analysis (~96 % of the land area in the NH).

The version of the CRUTS dataset we used (CRUTS3.10) included revised and updated P data (CRUTS3.10.01 precipitation). The PET estimates in this dataset were computed by the CRU using a variant of the Penman-Montieth equation (Montieth 1964; Shuttleworth 1993; Allen et al. 1994; Ekstrom et al. 2007; Sheffield et al. 2012). The PET equation used by the CRU is the grass reference evapotranspiration, developed by the Food and Agricultural Organization (FAO) (Allen et al. 1994); this defines PET from a clipped grass-surface 0.12 meters (m) in height and an assumed surface albedo of 0.23 (Ekstrom et al. 2007). This model computes PET based on monthly mean T, monthly mean minimum T, monthly mean maximum T, monthly mean vapor pressure and monthly mean cloud cover. Wind speed and temperature are direct outputs from the CRU model; net radiation, vapor pressure deficit and the slope of the vapor pressure curve are computed from the model output. Additionally, total cloud cover is estimated from long wave radiation computed by the HadRM3H model and is used to estimate the relative fraction of sunshine (i.e., sunshine hours per day divided by total day length) (Allen et al. 1994). Surface temperature (mean, minimum and maximum) and relative humidity are used to compute the vapor pressure deficit and the slope of the vapor pressure/temperature curve (Ekstrom et al. 2007). The CRUTS data are available for download at: http://iridl.ldeo.columbia.edu/SOURCES/.UEA/.CRU/.TS3p1/.monthly/, and documentation for the dataset is available at http://iridl.ldeo.columbia.edu/SOURCES/.UEA/.CRU/.TS3p1/.dataset_documentation.html.

The monthly CRUTS3.1 P and PET data were used with a monthly water-balance model to compute monthly deficit (D). The water-balance model includes the concepts of climatic water supply (i.e., P) and demand (i.e., PET), snow accumulation and melt, and soil-moisture storage (Wolock and McCabe 1999; McCabe and Markstrom 2007; McCabe and Wolock 2008). In the water-balance model, when precipitation for a month is less than PET, actual evapotranspiration (AET) is equal to P plus the amount of moisture that can be removed from the soil. The fraction of soil-moisture storage that can be removed decreases linearly with decreasing soil-moisture storage; that is, as the soil becomes drier water becomes more difficult to remove from the soil and less soil moisture is available for AET. When P exceeds PET in a given month, AET is equal to PET; water in excess of PET replenishes soil-moisture storage. When soil-moisture storage reaches capacity during a given month, the excess water becomes surplus, which eventually becomes runoff. The water-balance model also accounts for the accumulation and melting of snow in cold regions. Snow that melts is added to precipitation and is available for evapotranspiration, to recharge soil moisture storage, and/or to become surplus. Water deficit (D), the focus of this study, is computed as PET minus AET. Output from the water-balance model for the years 1905 through 2009 is used in the analysis; the output for 1901–1904 is excluded from the analyses because these first few years provide a "warm-up" period during which the model state variables equilibrate.

For details of the water-balance model see McCabe and Markstrom (2007). The model was not calibrated; rather, standard parameter values were used (see McCabe and Markstrom

2007). Similar water-balance models have been used successfully in other studies (Wolock and McCabe (1999); McCabe and Wolock (2008)).

3 Results and discussion

For most locations in the NH, mean monthly deficit is lowest (or zero) during cool season (October through March) months and highest during warm season (April through September) months (Fig. 1a). The highest values of mean monthly NH deficit generally occur during July and the lowest values generally occur during December or January. To examine these seasonal changes in more detail, the monthly values of deficit for each grid cell were converted to Z-scores. The monthly values for each grid cell were converted to Z-scores by

$$Z_{ij} = \frac{(X_{ij} - X_j)}{\sigma_j} \tag{1}$$

where Z_{ij} is the Z-score for year i and month j, X_{ij} is the raw deficit value for year i and month j, X_j is the long-term mean of X_{ij} for month j, and σ_j is the long-term standard deviation of X_{ij} for

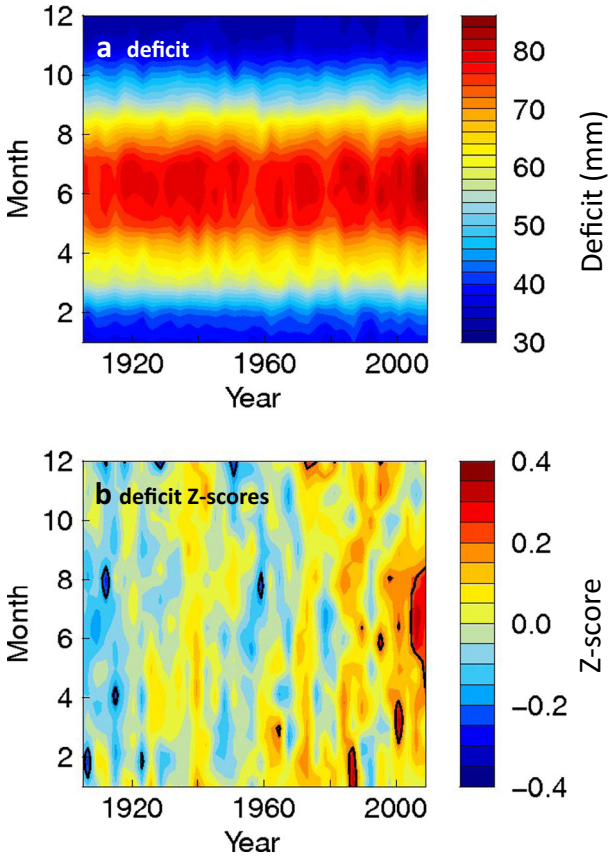

Fig. 1 Mean Northern Hemisphere **a** deficit, and **b** Z-scores of deficit. The *black lines* indicate deficit Z-scores that are less than the 5th percentile or greater than the 95th percentile

month *j*. Converting the raw values to Z-scores helps to more easily identify relative changes in deficit over time. Mean NH Z-scores of deficit (and other climatic and water balance variables) were computed as area-weighted averages.

An examination of mean NH Z-scores of deficit values indicates mostly negative Z-scores (i.e., wetter than the long-term average) for all months from 1905 to about 1920, and another period of primarily negative Z-scores from about 1940 to about 1970 (Fig. 1b). After about 2000, however, deficit Z-scores increased to mostly positive values (drier than the long-term average) for the months of February through September.

The temporal pattern of Z-scores for monthly T (Fig. 2b) resembles the temporal pattern of the Z-scores for the monthly water deficit (Fig. 1b); however, increases in T after about 2000 are larger than those for deficit and occur for all months of the year. The Z-scores for P (Fig. 2a) indicate smaller changes in monthly P compared to monthly T. Additionally, the Z-scores of P indicate an increase in P for almost all months after about 2000. This increase in NH P would be expected to decrease deficit values, but the increases in T apparently had a greater effect on changes in deficit after about 2000 than did the changes in P.

Another way to examine the changes in deficit, P, and T is to analyze changes across space through time. To do this, Z-scores of deficit, P, and T for the NH cool and warm seasons, and annually, were averaged by 5-degree latitudinal bands for each year during 1905–2009

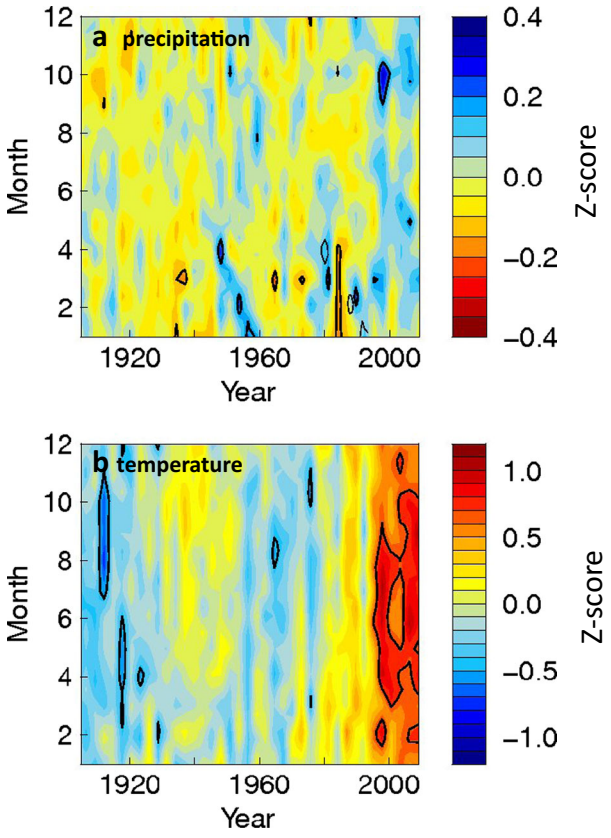

Fig. 2 Mean Northern Hemisphere Z-scores for **a** precipitation, and **b** temperature. The *black lines* indicate Z-scores that are less than the 5th percentile or greater than the 95th percentile

(Fig. 3). Temporal variability in cool season deficit appears to be largest for the 0° to 30°N latitudinal bands. In this geographic region, Z-scores of deficit values were largely negative until about 1920 and mostly positive after about 2000. For the warm season deficit, Z-scores are most variable for the 10°N to about 40°N latitudinal range. The region with the greatest variability in deficit values is located farther North in the warm season compared to the cool season because of the northward movement of the solar declination and weather systems during the NH warm season. The Z-scores of deficit for the warm season indicate primarily negative values before 1920 at middle latitudes and during about 1940 to about 1970 in the lower latitudes. In contrast, warm season Z-scores of deficit are mostly positive after about 2000. These results indicate that the mean NH changes in deficit Z-scores (Fig. 1b) are mostly driven by changes in deficit Z-scores for the 0° to about 40° latitudinal range (Fig. 3a and b). Dai (2013) also reported an increase in aridity around 1980, which is consistent with the temporal patterns in Fig. 3a and b. Our results, however, also show an even larger increase in deficit beginning around 2000.

The most notable signal in Z-scores of P for the cool and warm seasons (Fig. 3d and e) is mostly positive Z-scores for the 30° to 70°N latitudinal bands after about 1960. This relative increase in P appears to be associated with some decreases in deficit for the same latitudinal range and time period (Fig. 3a and b). Additionally, for the warm season there are relatively large positive P Z-scores between about 10° to 20°N during about 1950 to 1970 (Fig. 3e). These positive values of warm season P are consistent with decreased warm season deficit in this region during the same time period (Fig. 2b).

The latitudinal and temporal distributions of Z-scores for cool season and warm season T indicate similar patterns (Fig. 3g and h). The Z-scores of T for both seasons indicate nearly hemispheric negative Z-scores through the 1920s, and around 1970. Starting about 2000 there are nearly hemispheric positive Z-scores in T until the end of the period of record (Figs. 2b and 3g–i). The post 2000 period suggests a slowdown of the rate of global warming. This

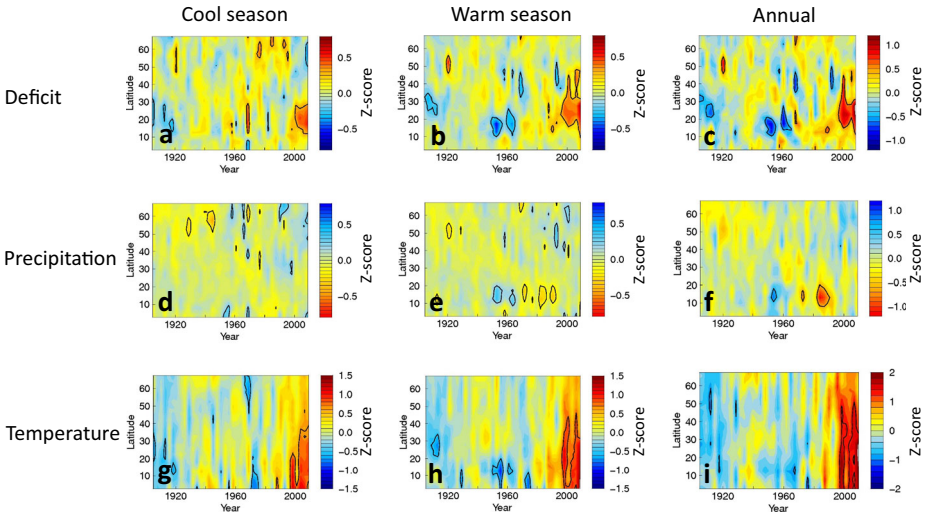

Fig. 3 Mean cool season (October through March), warm season (April through September), and annual Z-scores of deficit, precipitation, and temperature averaged for 5-degree latitudinal bands. The *black lines* indicate Z-scores that are less than the 5th percentile or greater than the 95th percentile

slowdown in the rate of global warming has been reported by a number of previous studies (Easterling and Wehner 2009; England et al. 2014; Meehl and Teng 2014). Meehl and Teng (2014) and England et al. (2014) suggest that cooling in the eastern tropical Pacific Ocean accounts for the slowing of the rate of warming, whereas Steinman et al. (2015) suggest that the warming slowdown is a result of a slight peak in the Atlantic Multidecadal Oscillation (AMO) (i.e., warm North Atlantic Ocean) and a negative Pacific Decadal Oscillation (PDO) (i.e., cool eastern tropical Pacific Ocean and warm north central Pacific Ocean). Additionally, Chen and Tung (2014) reported that the warming slowdown is related to a transport of surface heat to deep layers of the Atlantic Ocean and ocean areas near Antarctica (i.e., southern Oceans).

The variability in T Z-scores for the latitudinal bands from 0° to about 40°N (Figs. 3g and h) seem to co-vary with the deficit Z-scores for this range of latitudes (Fig. 3a and b). For the latitudes north of 40°N, the increases in T after about 2000 (Fig. 3g and h) did not result in large increases in deficit (Fig. 3a and b) because increases in P during this period (Fig. 3d and e) offset the increases in T. The combined effects of the cool season and warm season anomalies of deficit, P, and T appear to result in stronger anomalies in the annual data (Fig. 3c, f, and i).

Because deficit increased dramatically after about 2000, composite maps of mean Z-scores of cool and warm season deficit for the 2000–2009 period were computed to examine where in the NH the largest Z-scores in deficit occurred (Fig. 4a and b). In addition, composite maps of mean Z-scores for runoff (streamflow per unit area), P, and PET also were computed (Fig. 4c–h). Mean Z-scores for the 2000–2009 period that are statistically different ($p<0.05$) from mean Z-scores for 1905–1999 were plotted. The statistical significance of the mean Z-scores for 2000–2009 was computed using a Student's *t*-test. For the cool season, the most positive mean deficit Z-scores are for an area that stretches from northern Africa, through the Middle East into southern and central Asia (Fig. 4a). This same region shows large mean deficit Z-scores for the warm season (Fig. 4b). During the warm season an expanded area of positive deficit Z-scores also is evident for the western United States. The large area of positive Z-scores for the cool and warm seasons that stretches from northern Africa, through the Middle East into southern and central Asia (Fig. 4a and b) likely is the main cause of the positive Z-scores in NH deficit after about 2000 (Fig. 3a and b). The positive Z-scores in deficit appear to be related to positive Z-scores in PET (Fig. 4g and h). The correlation between the maps of deficit Z-scores and PET Z-scores are 1.0 for both the cool and warm season.

The patterns of Z-scores for runoff (Fig. 4c and d) and P (Fig. 4e and f) do not indicate much agreement with the patterns of Z-scores for deficit (Fig. 4a and b). The correlations between the maps of cool-season Z-scores for runoff (Fig. 4c) and P (Fig. 4e) with the map of cool season Z-scores for deficit (Fig. 4a) are 0.15 and 0.14, respectively. Whereas the correlations between the maps of warm-season Z-scores for runoff (Fig. 4d) and P (Fig. 4f) with the map of warm season Z-scores for deficit (Fig. 4b) are 0.05 and 0.10.

The maps of Z-scores for runoff (Fig. 4c and d) and P (Fig. 4e and f) do indicate some agreement with each other. The correlation between the maps of cool season runoff (Fig. 4c) and P (Fig. 4e) is 0.57 ($p<0.01$), and the correlation between the maps of warm season runoff (Fig. 4d) and P (Fig. 4f) is 0.76 ($p<0.01$).

The increase in NH deficit, especially just before 2000, reported in this study is consistent with Dai (2011) who reported that since the 1970s global aridity (based on PDSI) increased particularly in Africa, southern Europe, East and South Asia, and eastern Australia. Sheffield et al. (2012) also examined changes in the occurrence of global drought during 1950–2008

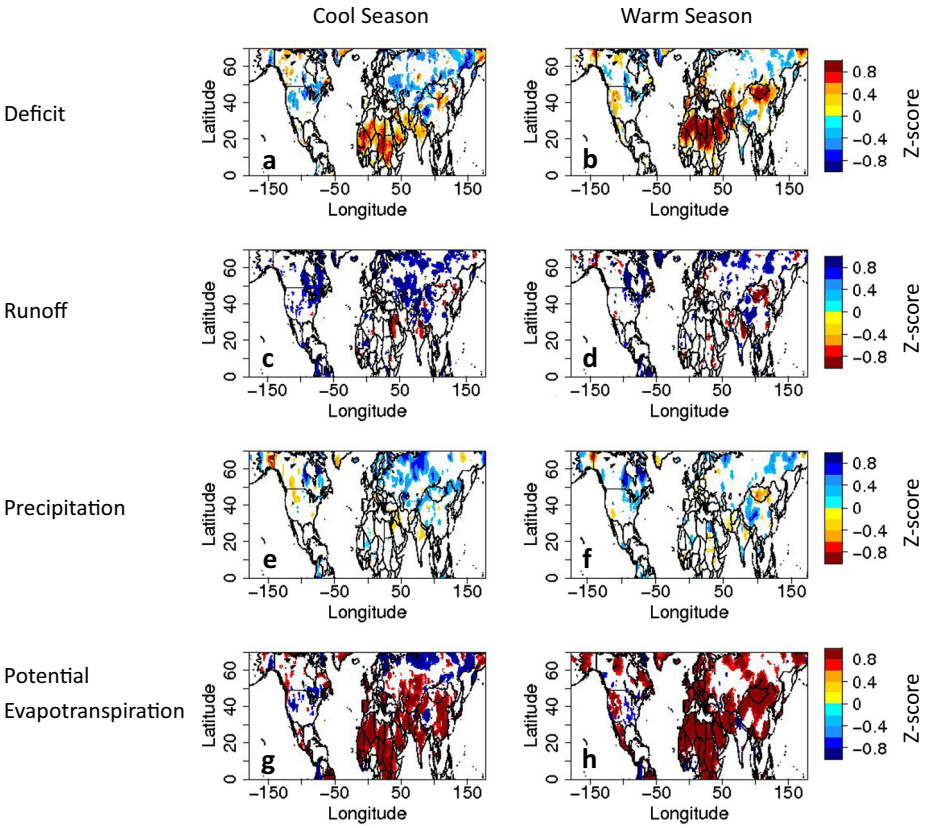

Fig. 4 Significant (at a 95% confidence level) changes in mean cool (October through March) and warm (April through September) season Z-scores of deficit, runoff, precipitation, and potential evapotranspiration for the period 2000–2009

using PDSI estimated in two ways: (1) based on the standard method using Thornthwaite PET (PDSI_TH), and (2) using Penman-Montieth PET (PDSI_PM). Their results indicated that drought occurrence over global land areas substantially increased during 1950–2008 when PDSI_TH values were analyzed. In contrast, when modified PDSI (computed using Penman-Montieth PET (PDSI_PM)) was examined there was only a small increase in drought over global land areas. The difference in the results was attributed to the greater sensitivity of Thornthwaite PET to temperature compared to the Penman-Montieth model. Sheffield et al. (2012) concluded that using Thornthwaite PET results in an over-estimate of drought. It should be noted that in our study, however, we used Penman-Montieth PET in the computation of deficit and still identified a substantial increase in NH deficit (i.e., aridity).

In an analysis of the global water balance, McCabe and Wolock (2014) found that global runoff increased after about 2000. This result seems to contradict the findings presented in this paper regarding changes in NH deficit. To examine this apparent contradiction, time series of runoff (estimated using the water-balance model) were analyzed. Similar to the other variables investigated, cool season, warm season, and annual time series of runoff for each NH CRUT

S3.1 grid cell were converted to Z-scores and then averaged to produce mean NH cool season, warm season, and annual runoff time series.

Comparisons of mean NH deficit and runoff time series (Fig. 5a–f) indicate near zero correlations for the annual (r=−0.03) and cool season (r=−0.04) times series, and a modest, although statistically significant (p<0.05), correlation for the warm season (r=−0.25). These correlations indicate that variability in deficit and runoff are mostly unrelated. A comparison of mean NH P and PET time series (Fig. 5g–l) with the deficit and runoff time series indicates correlations between deficit and PET of 0.69, 0.57, and 0.83 for the cool season, warm season, and annual time series respectively (all of these correlations are significant at p<0.01). Correlations between deficit and P are 0.23 (p<0.05), 0.19, and 0.04 for the cool season, warm season, and annual time series respectively. The correlations between deficit and P are much less significant than are the correlations between deficit and PET. These results indicate that variability in deficit is strongly controlled by variability in PET, and only weakly controlled by variability in P.

Correlations between the runoff and PET time series (Fig. 5) are 0.48 (p<0.01), 0.07, and 0.50 (p<0.01) for the cool season, warm season, and annual time series respectively, whereas correlations between seasonal and annual runoff with P are 0.63, 0.85, and 0.88 (all correlations are significant at p<0.01). These correlations indicate that although PET has some effect on runoff, P has a much greater effect on runoff than does PET, particularly during the warm season and annually.

The close relation between deficit and PET (and T) indicates a relation between global warming and increases in NH deficit. In addition to the effects of global warming on deficit, other factors also may influence the variability of deficit, such as sea-surface temperature variability (SST) (Steinman et al. 2015). A number of previous studies have indicated relations between the variability of NH hydroclimate and indices of sea-surface temperatures (SSTs) (Redmond and Koch 1991; Hoerling and Kumar 2003; McCabe and Palecki 2006; McCabe and Wolock 2008; Apipattanavis et al. 2009; Steinman et al. 2015).

To examine possible relations between NH deficit and SSTs we computed correlations between global annual SSTs and the time series of mean annual NH deficit. The SST indices we evaluated were: (1) NINO3.4 (SSTs averaged for the region 5° south (S) latitude to 5° (N) north (N) latitude and 170° west (W) longitude to 120° (W) west longitude; these SSTs are an index of the variability of the El Niño–Southern Oscillation (ENSO) (Trenberth 1997), (2) the AMO (SSTs averaged for the North Atlantic Ocean for the region 0° to 70°N latitude and 60°W to 10°W longitude), (3) Indian Ocean SSTs (ISST) (SSTs averaged for the Indian Ocean for 30°S latitude to 10°N latitude and 50° E longitude to 100° E longitude), and (4) the PDO.

The mean annual NINO3.4, AMO, and ISST time series were computed using monthly SST data from the Kaplan global SST dataset (Kaplan et al. 1998; http://iridl.ldeo.columbia.edu/SOURCES/.KAPLAN/.EXTENDED/.v2/.ssta/). The mean annual PDO data were computed from monthly PDO data obtained from (http://jisao.washington.edu/pdo/PDO.latest).

Correlations between the SST indices were computed using original (i.e., raw time series) and detrended time series. The time series were detrended to examine relations between NH deficit and SST time series due solely to inter-annual variability of SSTs and not influenced by long-term trends. The time series were detrended by removing long-term linear trends in the data time series.

Correlations between mean annual NH deficit and the SST index time series indicate statistically significant (at p<0.05) correlations for only the AMO and ISST (Table 1). The

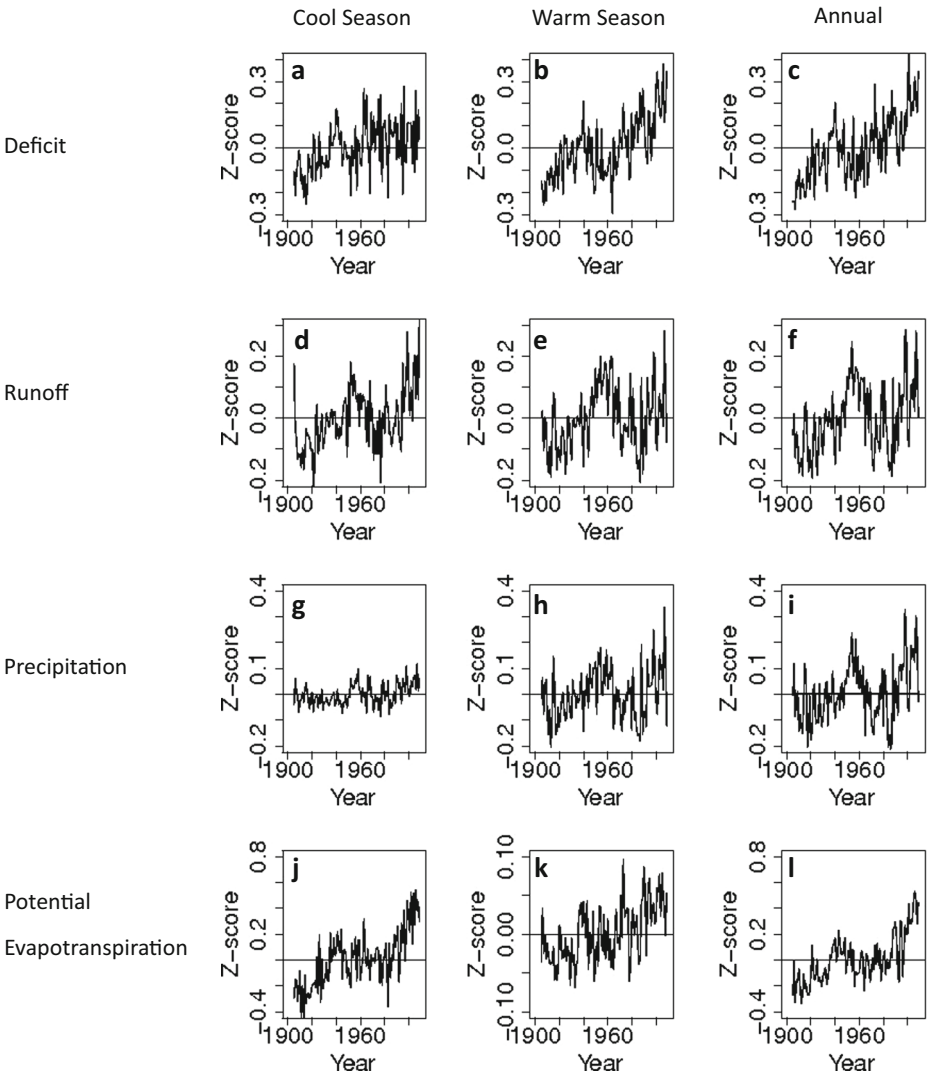

Fig. 5 Time series of mean Northern Hemisphere cool season (October through March), warm season (April through September), and annual Z-scores of deficit, runoff, precipitation, and potential evapotranspiration. The *horizontal lines* indicate the zero line. The range of Z-scores for potential evapotranspiration during the warm season is so small that a different y-axis was used for this graph (i.e., graph k) compared with the y-axes used for graphs j and i

correlations using the original time series are much larger than are the correlations using the detrended data. The larger correlations between AMO and ISST with mean annual NH deficit using the original time series compared with using the linearly detrended time series suggests that global warming has contributed to the long-term trends in all of these variables.

The relations between deficit and the AMO are consistent with previous research that showed a relation between these SSTs and drought (Hoerling and Kumar 2003; McCabe and Palecki 2006). Although the correlations computed using the detrended

Table 1 Correlations between original (i.e., raw) and detrended mean annual Northern Hemisphere deficit with original and detrended mean annual NINO3.4 sea-surface temperatures (SSTs) (NINO), Atlantic Multi-decadal Oscillation (AMO), Indian Ocean SSTs (ISST), and the Pacific Decadal Oscillation (PDO)

	Original	Detrended
NINO	0.06	−0.05
AMO	0.42[a]	0.19[a]
ISST	0.62[a]	0.27[a]
PDO	0.11	0.16

[a] indicates statistically significant correlations at a 95% confidence level

data are statistically significant for AMO and ISST, the correlations are relatively small and indicate that only a small amount of variance in mean annual NH deficit is explained by these SST indices.

For the period just before 2000, the mean NH time series of deficit and runoff indicate an increase in both deficit and runoff (Fig. 5a–f). At first glance this may seem counter-intuitive because one climatic variable (i.e., deficit) is indicating that the NH has become drier, whereas another climatic variable (i.e., runoff) is indicating that the NH has become wetter. The increase in NH runoff before about 2000 is consistent with previous research (McCabe and Wolock 2014), and the increase in deficit is consistent with previous research of trends in global PDSI and drought (Dai 2011; Sheffield et al. 2012).

These apparently contradictory results occur because deficit and runoff represent different components of the hydroclimate water and energy budget. In simple terms, deficit can be approximated as PET – AET, and runoff can be computed as P – AET. Thus, although AET is common to both of these climatic variables, deficit is largely controlled by PET and runoff is largely controlled by P. The large influence of P on runoff has been shown in previous research (McCabe and Wolock 2011). Since both PET (Fig. 5j–l) and P (Fig. 5g–i) increased before the year 2000, both deficit (Fig. 5a–c) and runoff (Fig. 5d–f) also increased.

The increase in runoff is an indication of increases in surface water supply in the NH. The increase in deficit is an indication of the potential for drying of soils in the NH. Where deficit has increased, additional irrigation will be needed for agriculture to keep soils from drying and to maintain crop yields. Although mean NH runoff (and related water supplies) has increased during recent years, this result does not reflect the effects of recent changes in climate on deficit and the potential effects of the changes in deficit on agriculture.

4 Conclusion

Monthly deficit computed using a water-balance model for grid cells across the NH indicates a substantial increase in deficit at about the year 2000. Deficit increased around 2000 during both the cool and warm NH seasons and the increases in deficit are related to a dramatic increase in T and PET at about 2000. Since 2000 deficit, T, and PET have remained at relatively high, but stable levels. The most notable increases in deficit occurred for the latitudinal band from 0° to 40°N. Even though T increased for all NH latitudes at about 2000, increases in precipitation for latitudes north of 40°N mitigated the effects of increases in T on deficit. The increase in T, PET, and deficit near 2000 are unprecedented during the 1905–

2009 period of study. The increases in deficit may already be having important implications for crop yields and vegetation distributions in the NH.

References

Allen RG, Smith M, Pereira LS, Perrier A (1994) An update for the calculation of reference evapotranspiration. ICID Bulletin 43:35–92

Apipattanavis S, McCabe GJ, Rajagopalan B, Gangopadhyay S (2009) Joint spatiotemporal variability of global sea surface temperatures and global Palmer drought severity index values. J Clim 22:6251–6267. doi:10.1175/2009JCLI2791.1

Arnell NW (2003) Effects of IPCC SRES emissions scenarios on river runoff: a global perspective. Hydrol Earth Syst Sci 7:619–641

Arora VK (2002) The use of the aridity index to assess climate change effect on annual runoff. J Hydrol 265: 164–177

Budyko MI (1948) Evaporation under natural conditions. Gidrometeorizdat, Leningrad, English translation by IPST, Jerusalem

Burke EJ, Brown SJ (2008) Evaluating uncertainties in the projection of future drought. J Hydrometeorol 9:292–299

Chen X, Tung K-K (2014) Varying planetary heat sink led to global-warming slowdown and acceleration. Science 345:897–903. doi:10.1126/science.1254937

Intergovernmental Panel on Climate Change (2014) Summary for Policymakers. In: Climate Change 2014: Impacts, Adaptation, and Vulnerability. Part A: Global and Sectoral Aspects. Contribution of Working Group II to the Fifth Assessment Report of the Intergovernmental Panel on Climate Change, Field CB, Barros VR, Dokken DJ, Mach KJ, Mastrandrea MD, Bilir TE, Chatterjee M, Ebi KL, Estrada YO, Genova RC, Girma B, Kissel ES, Levy AN, MacCracken S, Mastrandrea PR, and White LL (eds.), Cambridge University Press, Cambridge, United Kingdom and New York, NY, USA

Dai A (2011) Drought under global warming: a review. WIREs Clim Chang 2:45–65. doi:10.1002/wcc.81

Dai A (2013) Increasing drought under global warming in observations and models. Nat Clim Chang 3:52–58

Dai A, Trenberth KE, Qian T (2004) A global data set of palmer drought severity index for 1870–2002: relationship with soil moisture and effects of surface warming. J Hydrometeorol 5:1117–1130

Dobrowski SZ, Abatzoglou J, Swanson AK, Greenberg JA, Mynsberge AR, Holden ZA, Schwartz MK (2013) The climate velocity of the contiguous United States during the 20th century. Glob Chang Biol 19:241–251. doi:10.1111/gcb.12026

Easterling DR, Wehner MF (2009) Is the climate warming or cooling? Geophys Res Lett 36:L08706. doi:10.1029/2009GL037810

Ekstrom M, Jones PD, Fowler HF, Lenderink G, Buishand TA, Conway D (2007) Regional climate model data used within the SWURVE project 1: projected changes in seasonal patterns and estimation of PET. Hydrol Earth Syst Sci 11:1069–1083

England MH, McGregor S, Spence P, Meeh GA, Timmermann A, Cai W, Gupta AS, McPhaden MJ, Purich A, Santoso A (2014) Recent intensification of wind-driven circulation in the Pacific and the ongoing warming hiatus. Nat Clim Chang 4:222–227

Falkenmark M, Rockstrom J (2006) The new blue and green water paradigm: breaking new ground for water resources planning and management. J Water Res Pl-ASCE May/June, 129–132

Gleick PH (2000) Water: the potential consequences of climate variability and change for the water resources of the U.S. The Report of the Water Sector Assessment Team of the National Assessment of the Potential Consequences of Climate Variability and Change, Pacific Institute for Studies in Development, Environment, and Security, Oakland,
151

Hoerling MP, Kumar A (2003) The perfect ocean for drought. Science 299:691–694

Kaplan A, Cane M, Kushnir Y, Clement A, Blumenthal M, Rajagopalan B (1998) Analyses of global sea surface temperature 1856–1991. J Geophys Res 103:18,567–18,589

McCabe GJ, Markstrom SL (2007) A monthly water-balance model driven by a graphical user interface. U.S. Geological Survey Open-File report 2007–1088, 6 p

McCabe GJ, Palecki MA (2006) Multidecadal climate variability of global lands and oceans. Int J Climatol 26: 849–865. doi:10.1002/joc.1289

McCabe G, Wolock DM (2008) Joint variability of global runoff and global sea surface temperatures. J Hydrometeorol 9:816–824. doi:10.1175/2008JHM943.1

McCabe GJ, Wolock DM (2011) Independent effects of temperature and precipitation on modeled runoff in the conterminous United States. Water Resour Res 47:W11522. doi:10.1029/2011WR010630
McCabe GJ, Wolock DM (2014) Temporal and spatial variability of the global water balance. Clim Chang. doi:10.1007/s10584-013-0798-0
McDonald RI, Girvetz EH (2013) Two challenges for U.S. irrigation due to climate change: increasing irrigated area in wet states and increasing irrigation rates in dry states. PLoS ONE 8(6):e65589. doi:10.1371/journal.pone.0065589
Meehl GA, Teng H (2014) CMIP5 multi-model hindcasts for the mid-1970s shift and early 2000s hiatus and predictions for 2016–2035. Geophys Res Lett 41:1711–1716
Milly PCD, Dunne KA, Vecchia AV (2005) Global pattern of trends in streamflow and water availability in a changing climate. Nature 438:347–350. doi:10.1038/nature04312
Montieth JL (1964) Evaporation and environment. Symp Soc Exp Biol 19:205–234
Nijssen B, O'Donnell GM, Hamlet A, Lettenmaier DP (2000) Hydrologic sensitivity of global rivers to climate change. Clim Chang 50:515–517
Redmond KT, Koch RW (1991) Surface climate and streamflow variability in the western United States and their relationship to large scale circulation indices. Water Resour Res 27:2381–2399. doi:10.1029/91WR00690
Rind D, Goldberg R, Hansen J, Rosenzweig C, Ruedy R (1990) Potential evapotranspiration and the likelihood of future drought. J Geophys Res 95:9983–10004
Seager R, Ting M, Held I, Kushnir Y, Lu J, Vecchi G, Huang H-P, Harnik N, Leetmaa A, Lau N-C, Li C, Velez J, Naik N (2007) Model projections of an imminent transition to a more arid climate in southwestern North America. Science 316:1181–1184
Sheffield J, Wood EF (2008) Projected changes in drought occurrence under future global warming from multi-model, multi-scenario, IPCC AR4 simulations. Clim Dyn 31:79–105
Sheffield J, Wood EF, Roderick ML (2012) Little change in global drought over the past 60 years. Nature 491:435–440. doi:10.1038/nature11575
Shuttleworth WJ (1993) In: Maidment DR (ed) Handbook of hydrology. McGraw-Hill, New York, pp 4.1–4.53
Steinman BA, Mann ME, Miller SK (2015) Atlantic and Pacific multidecadal oscillations and Northern Hemisphere temperatures. Science 347:988–991
Stephenson N (1990) Climatic control of vegetation distribution: the role of the water balance. Am Naturalist 135:649–670
Stephenson NL (1998) Actual evapotranspiration and deficit: biological meaningful correlates of vegetation distribution across spatial scales. J Biogeogr 25:855–870
Trenberth KE (1997) The definition of El Niño. Bull Am Meteorol Soc 78:2771–2777
Wang GL (2005) Agricultural drought in a future climate: results from 15 global climate models participating in the IPCC 4th assessment. Clim Dyn 25:739–753
Weiskel PK, Wolock DM, Zarriello PJ, Vogel RM, Levin SB, Lent RM (2014) Hydroclimatic regimes: a distributed water-balance framework for hydrologic assessment and classification. Hydrol Earth Syst Sci Discuss 11:2933–2965. www.hydrol-earth-syst-sci-discuss.net/11/2933/2014/, doi:10.5194/hessd-11-2933-2014
Willmott CJ, Feddema JJ (1992) A more rational climatic moisture index. Professor Geogr 44:84–88. doi:10.1111/j.0033-0124.1992.00084.x
Wolock DM, McCabe GJ (1999) Effects of potential climatic change on annual runoff in the conterminous United States. J Am Water Resour Assoc 35:1341–1350